IPC

Indonesian Physics Communication

Department of Physics, Universitas Riau, Pekanbaru, Indonesia
p-ISSN 1412-2960 | e-ISSN 2579-521X

Vol. 22 | No. 3
November 2025

Web: https://kfi.ejournal.unri.ac.id
E-mail: kfi@ejournal.unri.ac.id

Design and electromagnetic simulation of rhombus-shaped split ring resonator metamaterials for telecommunication antenna applications

Saktioto[1,*], Yan Fatma Rizwan[1], Yan Soerbakti[1], Ari Sulistyo Rini[1], Syamsudhuha[2], Sofia Anita[3]

[1]Department of Physics, Universitas Riau, Pekanbaru 28293, Indonesia
[2]Department of Mathematics, Universitas Riau, Pekanbaru 28293, Indonesia
[3]Department of Chemistry, Universitas Riau, Pekanbaru 28293, Indonesia

*Corresponding author: saktioto@lecturer.unri.ac.id

ABSTRACT

This research presents the design, simulation, and characterization of rhombus-shaped split ring resonator (SRR) metamaterials integrated into microstrip antennas to enhance bandwidth and gain performance. The proposed metamaterial consists of one to four SRR unit cells fabricated using copper on an FR-4 substrate (ε_r = 4.3). Electromagnetic simulations were performed using CST Studio Suite within the 0.009 – 9 GHz frequency range, followed by post-processing and material parameter extraction using the Nicolson-Ross-Weir (NRW) method in MATLAB. The analysis revealed that the four-cell SRR configuration exhibited double-negative (DNG) behavior with relative permittivity ε_r = -96.21, relative permeability μ_r = -11.65, and refractive index n = -8.49. Integration of this metamaterial into the microstrip antenna resulted in significant performance enhancement, achieving a return loss of -48.31 dB, a bandwidth of 4.37 GHz, an operating frequency of 5.24 GHz, and a gain of 2.23 dBi. These results confirm that the rhombus SRR metamaterial structure effectively improves electromagnetic wave confinement and power transmission efficiency, demonstrating strong potential for advanced telecommunication and sensor applications.

Keywords: Metamaterial; microstrip antenna; rhombus; split ring resonator; telecommunication

Received 03-06-2025 | Revised 04-07-2025 | Accepted 05-08-2025 | Published 12-11-2025

INTRODUCTION

Metamaterials have attracted increasing attention from researchers worldwide in the last decade. Antenna technology has also experienced rapid development. The ability of antennas to transmit and receive information allows them to be applied in various important applications, such as telecommunications [1-4] and medicine [5-8].

The use of microstrip antennas remains a popular choice for researchers due to their small size, flat shape, and relatively low assembly costs. These antennas will be widely used in wireless communication systems in the future. They can provide higher bandwidth and gain than single microstrip antennas [9-12]. Artificial materials, now known as metamaterials, are widely used by researchers due to their unique properties and the ability to be tailored to their specific needs. Essentially, metamaterials are structures consisting of elements or cells that exhibit specific optical properties not found in nature [13-16]. Antenna parameters such as return loss, VSWR, bandwidth, gain, and directivity can be improved using metamaterials [17-20]. The type of metamaterial structure used is the split ring resonator (SRR) structure. The use of SRR structures allows for reduced size and can operate in multiple frequency bands, making them suitable for a wide range of applications [21-26]. Several studies have been conducted on circular [27], hexagonal [28], and square [29] metamaterial antennas.

This study designed and simulated a rhombic SRR metamaterial structure applied to a microstrip antenna. Variations of cells 1 – 4 were performed to observe the effect of additional cells on the parameters of the metamaterial and antenna. This research is expected to be a breakthrough in improving the parameters of microstrip antennas.

RESEARCH METHODS

Metamaterial Simulation and Characteristics

The metamaterial structure used is a rhombus with two separate metal rings. The design and simulation of the metamaterial structure were performed using the Computer Simulation Technology (CST) Studio Suite application program. The simulation data was processed using MATLAB. The materials used were copper as the patch (metal inclusion) and FR-4 as the substrate with an electrical constant of 4.3. The geometric dimensions and ring radii of the metamaterial structure are shown in Table 1. The metamaterial structure design used has four variations of SRR cells to compare the metamaterial characteristics. The metamaterial structure will be observed in the frequency range of 0.009 – 9 GHz.

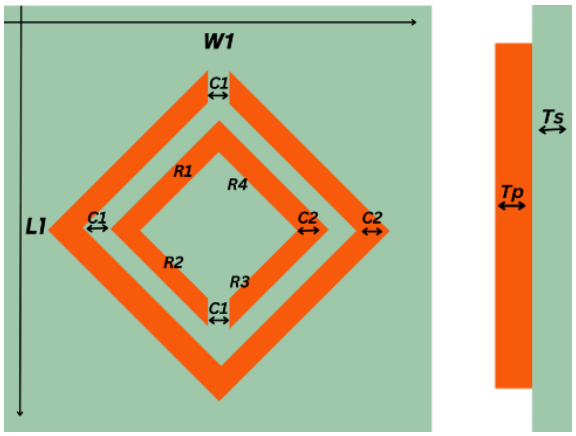

Figure 1. Front and side views of the rhombus-shaped SRR metamaterial structure design.

The initial design of the SRR metamaterial structure can be seen in Figure 1. The radius used is 3.5 mm and is the same for each cell variation. The geometric dimensions of the metamaterial structure can be seen in Table 1.

Table 1. Dimensions of the SRR metamaterial.

Symbol	Size (mm)
C_1	0.43
C_2	0.6
T_S	1.6
T_P	0.035
L_1	7.4
W_1	2.14

Electromagnetic wave ports with perfect electric (PEC) and magnetic (PMC) boundary conditions were applied to the metamaterial structure to obtain S-parameters through full-wave simulation. Characterization was performed using the Nicolson-Ross-Weir (NRW) method to extract effective electromagnetic parameters. The S11 (reflection) and S21 (transmission) data, in magnitude and phase, were then converted into complex form using the following equations:

$$S_{11} = |S_{11}|e^{i\theta_{11}} \quad (1)$$

$$S_{21} = |S_{21}|e^{i\theta_{21}} \quad (2)$$

The relative permittivity (ε_r) and relative permeability (μ_r), and the refractive index (n) were calculated using MATLAB based on the following NRW equation:

$$V_1 = S_{21} + S_{11} \quad (3)$$

$$V_2 = S_{21} - S_{11} \quad (4)$$

$$k = \frac{2}{jt_m}\frac{(1-V_1)(1+\Gamma_1)}{1-\Gamma_1 V_1} \quad (5)$$

$$\mu_r = \frac{2}{jk_0 t_m}\frac{1-V_2}{1+V_2} \quad (6)$$

$$\varepsilon_r = \frac{2}{jk_0 t_m}\frac{1-V_1}{1+V_1} \quad (7)$$

where, $k_0 = 2\pi f/c$, where f is the frequency used and c is the speed of light (3×10^8 m/s). The t_m value indicates the distance between the input and output excitation channels within the SRR metamaterial structure.

Metamaterial Antenna Design

The design and simulation of an antenna structure using a combination of rhombic metamaterials and four SRR variations were performed using CST Studio Suite software. The design of this metamaterial combination antenna structure is shown in Figure 2.

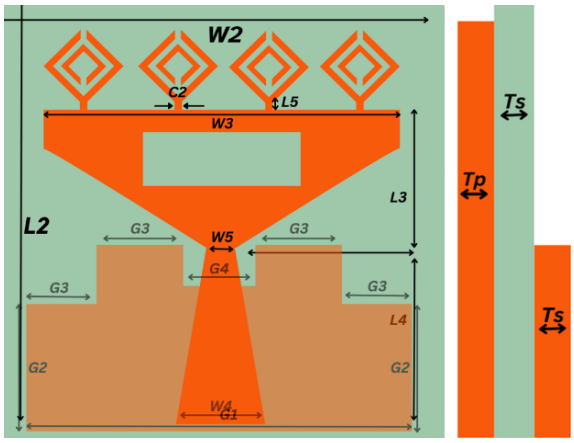

Figure 2. Front, rear, and side views of the SRR metamaterial antenna structure.

The antenna used is a microstrip antenna consisting of a substrate, patch, and ground elements. This antenna structure is made of copper for the patch and FR-4 for the substrate. The geometric dimensions of the metamaterial antenna are listed in Table 2. This metamaterial antenna structure has undergone several optimization stages to achieve optimal antenna performance.

Table 2. Dimensions of the metamaterial combination antenna structure.

Symbol	Size (mm)	Symbol	Size (mm)
C_2	1	W_4	2.14
L_2	33.34	W_5	1
L_3	5.8	G_1	29.60
L_4	13.2	G_2	7.4
L_5	0.6	G_3	7.4
W_2	29.60	G_4	3.94

RESULTS AND DISCUSSION

Metamaterial Structure Characteristics

The SRR metamaterial structure with four cell variations produces DNG (Double Negative) material characteristics, which are analyzed by processing S-parameter data, namely S11 (reflection spectrum) and S21 (transmission spectrum), using the NRW equation. These metamaterial characteristics include relative permittivity, relative permeability, and refractive index, as shown in Figures 3, 4, and 5.

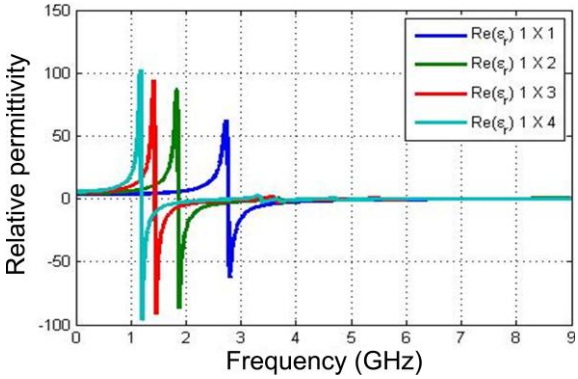

Figure 3. Effect of cell variations on the relative permittivity of the metamaterial.

The relative permittivity graph shows that the metamaterial structure with a combination of four cells has a higher negative permittivity value than other combinations. The maximum permittivity resonance reaches -96 at an operating frequency of 1.197 GHz.

The change in the graph from 1×1 to 1×4 reflects how the complexity and interactions within the structure affect its electromagnetic response. Increasing the number of elements increases the complexity of electromagnetic field interactions, which is reflected in changes in relative permittivity at various frequencies. As the number of elements increases, the interactions between the elements also increase. This can affect the distribution of electric and magnetic fields within the structure, which in turn affects the relative permittivity.

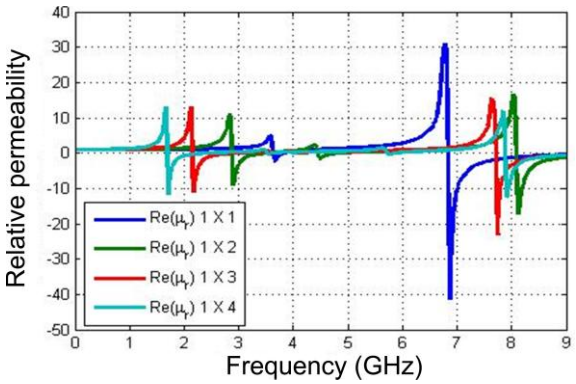

Figure 4. Effect of cell variations on the relative permeability of metamaterial structures.

Figure 4 shows a graph of relative permeability. The combination of four cells in the SRR metamaterial structure produces a higher negative permeability value than other

combinations. The resulting maximum permeability resonance is -11.65 at an operating frequency of 1.71 GHz. The graph above shows how the addition of elements in a material or antenna configuration affects its magnetic properties, indicated by changes in relative permeability. Each configuration has a unique resonance pattern that reflects the complex interactions between the elements in the structure. These changes are useful for applications in communication antenna device design, where precise control over the material's electromagnetic properties is essential.

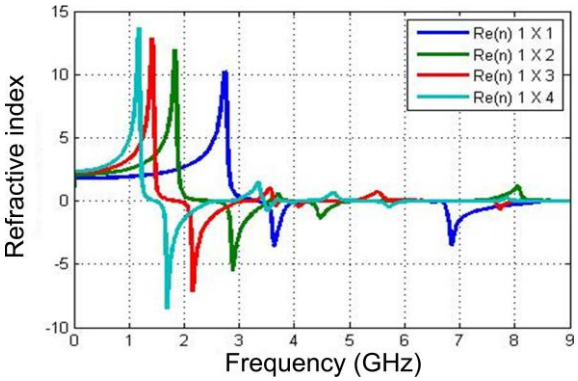

Figure 5. Effect of cell variations on the refractive index of metamaterial structures

Figure 5 shows a graph of the refractive index. The combination of four cells in the SRR metamaterial structure produces a maximum refractive index of -8.49 at an operating frequency of 1.69 GHz. The refractive index value is obtained from the previously obtained permittivity and permeability values. The shift in the resonant frequency of the refractive index occurs due to the addition of cells to the metamaterial structure.

Metamaterial Antenna Performance

The metamaterial combination microstrip antenna with a variation of 4 SRR cells produces good performance. Antenna parameters include return loss, VSWR, gain, and directivity. Figure 6 shows that metamaterial combination antennas with variations of 1 – 4 SRRs produce a significant change in return loss. The highest return loss value occurs for the 3-cell variation antenna, at -52.99 dB. This indicates less power loss in the transmission process, thus improving antenna performance.

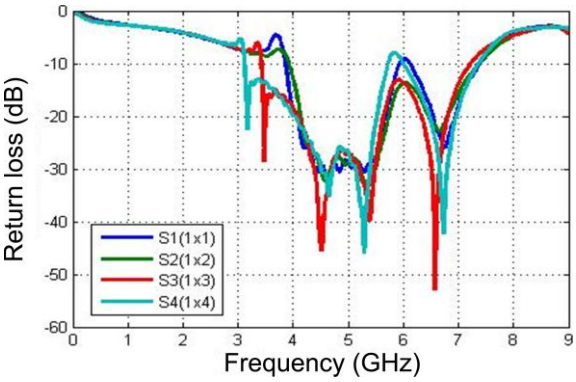

Figure 6. Comparison of return loss values for metamaterial antennas with cell variations.

Figure 7 shows the VSWR values for the 1 – 4 SRR combination antenna. The VSWR value can be seen in index 1.

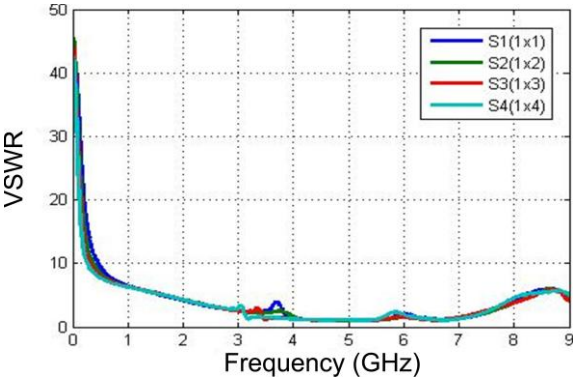

Figure 7. Comparison of VSWR values for metamaterial antennas with cell variations.

Figure 8 shows the gain pattern of each cell variation, which changes over the frequency range from 0.45 GHz to 3.17 GHz.

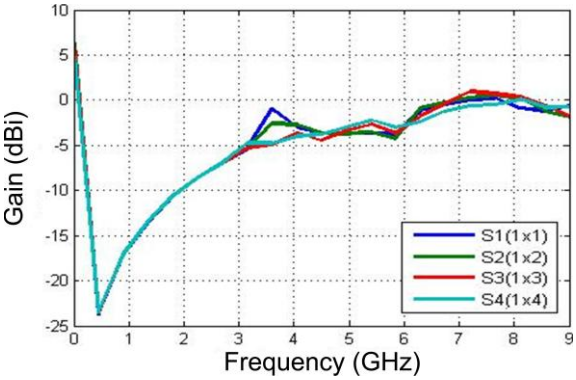

Figure 8. Comparison of the gain values of the metamaterial antenna with the cell variations.

This change occurs due to the interaction of the metamaterial structure with the SRR combination applied to the antenna when power flows through the attached metamaterial structure.

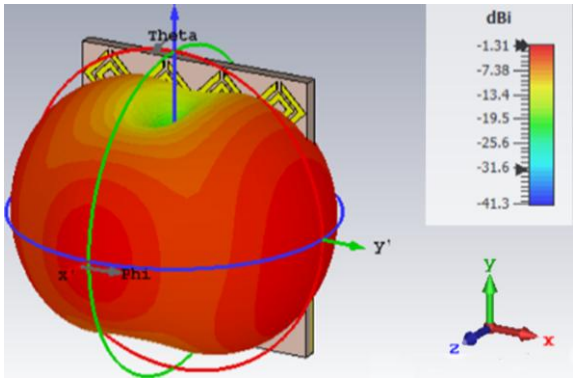

Figure 9. Change in radiation pattern of the 4-cell metamaterial antenna.

Figure 9 shows the radiation pattern for the 4-cell SRR combination metamaterial antenna. The antenna's radiation pattern is omnidirectional, with the antenna's maximum radiation point located in front of the structure.

CONCLUSION

The metamaterial structure of 4 SRR cell variations produces better metamaterial characteristics than other combinations with a relative permittivity (ε_r) of -96, a relative permeability (μ_r) of -11.65 and a refractive index (n) of -8.49. The use of metamaterial structures in microstrip antennas has been shown to improve antenna parameters. This study shows that antennas with a combination of 4 SRR cell metamaterials have great potential for telecommunication sensor applications, with a return loss value of -48.31 dB, an operating frequency of 5.24 GHz, a bandwidth of 4.37 GHz, and a gain of 2.23 dBi.

ACKNOWLEDGMENTS

This research was supported by the RIIM program, funded by BRIN and LPDP under Contract 72/IV/KS/05/2023 and 10511/UN19. 5.1.3/AL.04/2023. The authors sincerely thank both institutions for their continued support in the second-year funding (2025).

REFERENCES

1. Schmidt, R. & Webb, A. (2017). Metamaterial combining electric-and magnetic. *ACS Appl. Mater. Interfaces*, **9**.
2. Defrianto, D., Saktioto, S., & Emrinaldi, T. (2024). Analysis and modelling of the characteristics of telecommunication antennas utilising metamaterials with a circular structure. *Indones. Phys. Commun.*
3. Defrianto, D., Saktioto, S., Anita, S., Zahroh, S., & Soerbakti, Y. (2024). Perancangan dan simulasi antena telekomunikasi berdasarkan karakteristik metamaterial struktur lingkaran. *Prosiding Seminar Nasional Fisika Universitas Riau Ke-IX (SNFUR-9)*, **9**(1), 1002.
4. Saktioto, S., Siregar, F. H., & Anita, S. (2024). Excellent integration of a multi-SRR-hexagonal DNG metamaterial into an inverted triangle top microstrip antenna for 5G technology applications at 3.5 GHz. *Przeglad Elektrotechniczny*, **2024**(1), 130.
5. Tao, Y., Yang, E., & Wang, G. (2017). Left-handed metamaterial lens applicator. *Appl. Comput. Electromagn. Soc. J.*, **32**.
6. Saktioto, S., Angraini, C. Y. T., Soerbakti, Y., Rini, A. S., Syamsudhuha, S., & Anita, S. (2025). Design and optimization of square SRR metamaterial-based microstrip antenna for wideband biomedical sensing. *Science, Technology, and Communication Journal*, **6**(1), 7–16.
7. Amalia, R., Saktioto, S., & Soerbakti, Y. (2024). Simulasi dan analisis sifat metamaterial struktur segitiga pada frekuensi gelombang mikro untuk aplikasi sensor medis. *Prosiding Seminar Nasional Fisika Universitas Riau Ke-IX (SNFUR-9)*, **9**(1), 1001.
8. Amalia, R., Defrianto, D., & Abdullah, H. Y. (2024). Simulation and analysis of triangular structure metamaterial properties at microwave frequencies for medical

sensor applications. *Sci. Technol. Commun. J.*, **5**(1), 15–20.
9. Lai, A., Leong, K. M., & Itoh, T. (2007). Infinite wavelength resonant antennas. *IEEE Trans. Antennas Propag.*, **55** (3).
10. Angraini, C. Y. T., Saktioto, S., & Soerbakti, Y. (2024). Rancangan dan simulasi metamaterial struktur persegi empat sebagai aplikasi antena. *Prosiding Seminar Nasional Fisika Universitas Riau Ke-IX (SNFUR-9)*, **9**(1), 1003.
11. Rizwan, Y. F., Saktioto, S., & Soerbakti, Y. (2024). Perancangan struktur metamaterial segi empat pada frekuensi GHz untuk aplikasi antena mikro. *Prosiding Seminar Nasional Fisika Universitas Riau Ke-IX (SNFUR-9)*, **9**(1), 1004.
12. Soerbakti, Y., Defrianto, D., & Asyana, V. (2023). Performance analysis of metamaterial antennas based on variations in combination and radius of hexagonal SRR. *Sci. Technol. Commun. J.*, **4**(1), 1–4.
13. Goswami, S., Sarmah, K., & Baruah, S. (2016). Slot loaded square patch antenna with CSRR at ground plane. *MicroCom*, 1.
14. Soerbakti, Y., Gamal, M. D. H., & Syahputra, R. F. (2024). Negative refractive index anomaly characteristics of SRR hexagonal array metamaterials. *Sci. Technol. Commun. J.*, **4**(2), 63–68.
15. Gamal, M. D. H., Soerbakti, Y., & Saktioto, S. (2020). Investigasi karakteristik anomali indeks bias negatif metamaterial array struktur split ring resonator. *Prosiding SNFUR-5*, **5**(1), 1010.
16. Syahputra, R. F., Soerbakti, Y., & Saktioto, S. (2020). Effect of stripline number on resonant frequency of hexagonal split ring resonator metamaterial. *J. Aceh Phys. Soc.*, **9**(1), 26.
17. Kumar, A., Gupta, N., & Gautam, P. C. (2016). Gain and bandwidth enhancement techniques. *Int. J. Comput. Appl.*, **148**(7).
18. Saktioto, S., Soerbakti, Y., & Okfalisa, O. (2022). Improvement of low-profile microstrip antenna performance by hexagonal. *Alex. Eng. J.*, **61**(6), 4241.
19. Defrianto, D., Soerbakti, Y., & Saktioto, S. (2020). Analisis kinerja antena berdasarkan pengaruh variasi kombinasi. *Prosiding SNFUR-5*, **5**(1), 1004.
20. Soerbakti, Y., Syahputra, R. F., & Gamal, M. D. H. (2020). Investigasi kinerja antena berdasarkan dispersi anomali metamaterial. *Komunikasi Fisika Indonesia*, **17**(2), 74.
21. Suci, D. N. & Muldarisnur, M. (2021). Optimasi filter gelombang mikro berbasis metamaterial. *Jurnal Fisika Unand*, **10**(2).
22. Defrianto, D. Saktioto, S., & Soerbakti, Y. (2025). Exploration of analyte electrolyticity using multi-SRR-hexagonal dng metamaterials and ZnO thin films. *Indones. J. Electr. Eng. Inform.*, **13**(2).
23. Saktioto, S., Soerbakti, Y., & Rati, Y. (2024). Extreme DNG metamaterial integrated by multi-SRR-square and ZnO thin film for early detection of analyte electrolyticity. *Przeglad Elektrotechniczny*.
24. Saktioto, S., Soerbakti, Y., & Rati, Y. (2024). Effectiveness of adding ZnO thin films to metamaterial structures as sensors. *Indonesian Physics Communication*, **21**(1).
25. Soerbakti, Y., Saktioto, S., & Rati, Y. (2024). Optimization of semiconductor-based SRR metamaterials as sensors. *Journal of Physics: Conference Series*.
26. Soerbakti, Y., Saktioto, S., & Rini, A. S.. (2022). A review - Integrasi lapisan tipis ZnO pada aplikasi metamaterial sebagai wujud potensi sensor ultra-sensitif dan multi-deteksi. *Prosiding SNFUR-7*, **7**(1).
27. Jacob, J. K., Vasudevan, D., & Paul. B. J. (2019). Miniaturization of patch antenna using SRR and CSRR. *Int. Res. J. Eng. Technol.*, **6**(6), 870–874.
28. Buragohain, A., Das, G. S., & Doloi, T. (2023). Highly sensitive differential hexagonal split ring resonator sensor. *Sens. Actuators A: Phys.*, **363**, 114704.
29. Dong, Y. & Itoh, T. (2012). Metamaterial-based antennas. *Proc. IEEE*, **100**(7), 2271.